Epoxy–Aromatic Diamine Kinetics. 1. Modeling and Influence of the Diamine Structure

E. Girard-Reydet,† C. C. Riccardi,‡ H. Sautereau,† and J. P. Pascault*,†

Laboratoire des Matériaux Macromoléculaires, URA CNRS No. 507, Institut National des Sciences Appliquées de Lyon, 20 Avenue A. Einstein, 69621 Villeurbanne Cedex, France, and Institute of Materials Sciences and Technology (INTEMA), University of Mar del Plata and National Research Council (CONICET), J. B. Justo 4302, 7600 Mar del Plata, Argentina

Received March 20, 1995; Revised Manuscript Received July 12, 1995⊗

ABSTRACT: The reactivities of different aromatic diamines, i.e. 4,4′-diaminodiphenyl sulfone (DDS), 4,4′-methylenedianiline (MDA), 4,4′-methylenebis[2,6-diethylaniline] (MDEA), and 4,4′-methylenebis[3-chloro-2,6-diethylaniline] (MCDEA), cured with an epoxy prepolymer, the diglycidyl ether of Bisphenol A (DGEBA), were compared and correlated to their chemical structures. The reactivities of the diamines are in the following order: MDA > MDEA > DDS > MCDEA. Although MDA, MDEA, and MCDEA exhibit very different reactivities, the ratio of the reactivity of secondary to primary amine hydrogens (k_2/k_1) is found to be the same $r = 0.65$. On the other hand, the reactivity ratio of DDS is found to be $r = 0.45$. This lower value may be the result of the lower number of stable conformations afforded by the $-SO_2-$ group in comparison to the $-CH_2-$ group. No temperature dependence was observed. The DGEBA–DDS and DGEBA–MCDEA kinetics were fully characterized as regards conversions and T_g measurements with time at different temperatures. Relationships between the T_g and x were validated for both systems. Kinetics were modeled throughout the whole range of cure. For the DGEBA–MCDEA system, etherification reactions were found to occur and were then integrated into the kinetic model. The effect of diffusion control was incorporated by modifying the overall rate constant according to the Rabinovitch model. The Adam–Gibbs theory was preferred to express the temperature dependence of the diffusion rate constant. The kinetic models have been satisfactorily extended to the isothermal cure of an epoxy with a binary mixture of diamines.

Introduction

The mechanism and kinetics of the epoxy–amine curing reaction have been widely analyzed.[1–8] Three principal reactions take place:

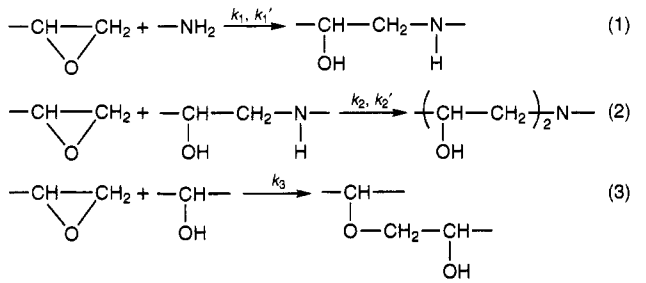

(1)

(2)

(3)

Step 1 illustrates the reaction of the primary amine hydrogen with the epoxy group. This is followed by the secondary amine hydrogen reacting with another epoxy group (step 2). Although a single activation energy and heat of reaction are experimentally obtained for both steps, reactivities of the primary and secondary amino groups may be different. Evaluation of the ratio of the rate constants $r = k_2/k_1$ was the subject of many studies.[1,3–5,8–20] This ratio is indeed supposed to have a strong effect on the cure process. Unfortunately, there is generally disagreement in the literature concerning the values obtained. Moreover, as the ratio is generally reported to be temperature independent,[1,4,8] some authors[13–14] found an increasing trend with cure temperature.

The tendency of the etherification reaction (step 3) to take place depends on the temperature[3,18] and the basicity of the diamine[21] and increases with the initial ratio of epoxy/amine.[3]

It is generally accepted that the curing reaction occurs by two competitive mechanisms:[1,5] one is catalyzed by the hydroxyl groups initially present in the epoxy prepolymer and those generated during the reaction (rate constants k_1, k_2), and the other is a noncatalytic mechanism (rate constants k_1, k_2) identified by a second-order reaction. The catalytic mechanism vanishes at high temperatures due to the difficulty of forming the ternary transition complex, whereas the noncatalytic reaction takes place over the whole temperature range. Rozenberg[6] showed, in fact, using highly pure reactants, that the noncatalyzed reactions do not really occur and that nucleophilic addition on the epoxy ring proceeds with the preliminary activation of the epoxy ring by amines, which act both as an electrophilic and as a nucleophilic agent. However, both kinetic treatments can be used for the description of epoxy–amine cure reactions because they lead to the same kinetic constants and activation energies.

In the early stage of curing, i.e. when T_g is well below the cure temperature T_{cure}, the kinetics are mainly controlled by the rate of the chemical reaction. At higher conversion and after vitrification, the reactions become diffusion controlled. Therefore to model the reaction throughout the whole range of the cure, the diffusion control mechanism must be taken into account. It has been shown that an excellent description of the diffusion process can be carried out for thermosets using glass transition theories.[19–20,22–25]

In this work, reaction kinetics were studied for a classical epoxy prepolymer, the diglycidyl ether of Bisphenol A, DGEBA, reacted with various aromatic diamines: 4,4′-diaminodiphenyl sulfone (DDS), 4,4′-

* To whom correspondence should be addressed.
† Institut National des Sciences Appliquées de Lyon.
‡ University of Mar del Plata and National Research Council.
⊗ Abstract published in *Advance ACS Abstracts,* October 15, 1995.

0024-9297/95/2228-7599$09.00/0

Table 1. Characteristics of the Different Monomers Used

Monomers	Formula	Supplier	Molar mass (g mol^{-1})	Melting temperature (°C)
4,4'-diaminodiphenylsulfone (DDS)	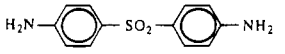	Fluka	238	175
4,4'-methylenedianiline (MDA)	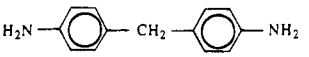	Fluka	198	88
4,4'-methylenebis[2,6-diethylaniline] (MDEA)	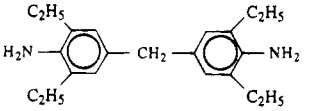	Lonza	310.5	88
4,4'-methylenebis[3-chloro 2,6-diethylaniline] (MCDEA)	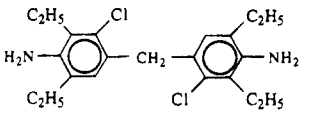	Lonza	380	92
diglycidyl ether of bisphenol A (DGEBA) i = 0.03	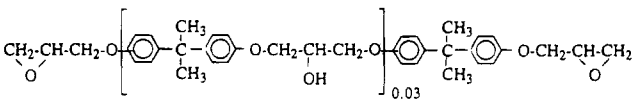	Dow Chemicals DER 332	348.5	47

methylenedianiline (MDA), 4,4'-methylenebis[2,6-diethylaniline] (MDEA), and 4,4'-methylenebis[3-chloro-2,6-diethylaniline] (MCDEA) (cf. Table 1). The study is mainly based on DDS and MCDEA; MDA and MDEA were introduced in order to understand the effect of the diamine structure on kinetics and properties. Owing to controversies in the existing r values, the ratios of the rate constants were also considered. A full description of cure kinetics (prior to and after vitrification) will be given.

Experimental Section

Materials. The chemical structures and characteristics of the different monomers are listed in Table 1.

All reactants were used as received with stoichiometric ratios equal to 1. The curing agents were first mixed with the epoxy prepolymer at 135 °C for DDS and 90 °C for the others. Minimum reaction occurs during this step, as confirmed by chromatographic measurements (conversions just after mixing are found less than 3%).

Technique. Kinetic studies were conducted in a regulated oil bath at various temperatures. Samples, placed in culture tubes, were removed from the bath after selected time intervals and studied by differential scanning calorimetry (DSC) and size exclusion chromatography (SEC) or high-pressure liquid chromatography (HPLC). DSC analysis was carried out in a Mettler TA3000 apparatus under an argon atmosphere. Measurements of the glass transition temperature, T_g, and heat capacity change at T_g, ΔC_p, were conducted at a heating rate of 10 °C·min^{-1}. The vitrification time was experimentally defined as the time at which an exothermic physical aging peak appears. To erase the influence of the physical aging on T_g measurements, samples were heated to a temperature just beyond the observed T_g, then cooled rapidly, and heated a second time to determine the T_g.[26]

SEC and HPLC were employed to estimate the extent of the reactions.

From analysis of the soluble products (extracted in tetrahydrofuran THF), SEC was actually found to be a suitable method to follow the conversion of DGEBA monomer, X_e, and both DDS and MCDEA monomers, X_a. A Waters chromatograph was used with double detection (UV at $\lambda = 254$ nm and a differential refractometer). The eluent used was THF, and the separation was carried out on four μ-Styragel columns (10^3 Å + 500 Å + 100 Å + 100 Å) with a flow rate of 1 mL·min^{-1}.

The disappearance of epoxy, X_e, and diamine, X_a, monomers can be followed using

$$X_e = 1 - \left(\frac{h_t}{h_0}\right)_e \quad (4)$$

$$X_a = 1 - \left(\frac{h_t}{h_0}\right)_a \quad (5)$$

where h_t/h_0 is the ratio of the actual height of the peak with respect to the initial one.

The extent of reaction was determined by following the epoxy monomer conversion, X_e. As both epoxides have equal reactivities (no substitution effect), the fraction of unreacted DGEBA at a certain epoxy conversion, x_e, is given by the simultaneous probability that both epoxy groups remain unreacted:

$$(1 - X_e) = (1 - x_e)^2 \quad (6)$$

Equations 4 and 6 lead to

$$x_e = 1 - \left(\frac{h_t}{h_0}\right)^{1/2} \quad (7)$$

SEC elution times related to DGEBA and both MDEA and MDA comonomers were found to be nearly the same. HPLC was then used to separate these monomer peaks. The components of the apparatus were a Waters 600E system controller, a Waters novapak C_{18} column and a Waters 486 tunable absorbance UV detector. The mobile phase was 70% acetonitrile/30% water for DGEBA–MDEA and 60% acetonitrile/40% water for DGEBA–MDA. The flow rate was 1 mL·min^{-1}, and the UV detector was set to 254 nm. Conversions were determined by following on HPLC chromatographs the ratio of the actual area peak with respect to the initial one (S_t/S_0). The X_e, X_a, and x_e values can thus be obtained by eqs 4–7 with S_t/S_0 instead of h_t/h_0.

The gelation time is considered to be the time at which the presence of an insoluble fraction in THF is first observed.

Molecular modeling was achieved using Tripos' Sybyl 6.0. software running on a IBM 6000 remote machine. The grid search procedure was run as available in the search module. For the minimization, the force field parameters for minimum 2 were modified as follows: ⟨⟨maximum iterations⟩⟩ was set at 10 000, and ⟨⟨simplex iterations⟩⟩, at 50. Unless otherwise stated, the other parameters were set to default.

Background

Determination of the Reactivity Ratio, $r = k_2/k_1$. The kinetic scheme of the curing of a diepoxy with a diamine is illustrated in Figure 1. On this basis and assuming that (i) the reactivities of the epoxy groups are independent, (ii) the ratio r does not depend on conversion, (iii) no etherification occurs, and (iv) both

catalytic (k_1, k_2) and noncatalytic (k'_1, k'_2) mechanisms are involved, a series of differential equations, as described by Dusek et al.,[2] may be written:

$$\left.\begin{aligned}
-\frac{dA_0}{dt} &= 4A_0E(k_1[OH] + k'_1)\\
-\frac{dA_1}{dt} &= E\{A_1\{(2k_1[OH] + 2k'_1) +\\
&\quad (k_2[OH] + k'_2)\} - 4A_0(k_1[OH] + k'_1)\}\\
-\frac{dA_2}{dt} &= 2E\{A_2(k_2[OH] + k'_2) - A_1(k_1[OH] + k'_1)\}\\
-\frac{dA'_2}{dt} &= E\{A'_2(2k_1[OH] + 2k'_1) - A_1(k_2[OH] + k'_2)\}\\
-\frac{dA_3}{dt} &= E\{A_3(k_2[OH] + k'_2) + A'_2(k_1[OH] + k'_1) -\\
&\quad A_2(2k_2[OH] + 2k'_2)\}\\
-\frac{dA_4}{dt} &= -EA_3(k_2[OH] + k'_2)
\end{aligned}\right\} \quad (8)$$

where E is the concentration of unreacted epoxy, [OH] is the concentration of hydroxyl groups, and A_i is the concentration of diamine with i as the number of reacted amine hydrogens.

The set of differential equations may be solved by dividing all the equations by the first one, thus eliminating the dependence on time.

If it is assumed that $r = k_2/k_1 = k'_2/k'_1$, the conversion of amino-hydrogen groups x_a (equal to x_e for a stoichiometric mixture) can then be written in terms of A_0 and r only, as follows:

$$x_a = 1 - \frac{1}{2 - r}\{(1 - r)A_0^{1/2} + A_0^{r/4}\} \quad (9)$$

At different curing times, x_a and A_0 can be determined experimentally by SEC or HPLC measurements:

$$x_a = x_e \text{ with } x_e \text{ defined by eq 7}$$

$$A_0 = 1 - X_a \text{ with } X_a \text{ defined by eq 5}$$

Determination of the Chemical Kinetic Constants. Considering the previously described epoxy–amine reaction paths, the following kinetic equations may be written

$$-\frac{de}{dt} = e\{[k'_1 + k_1(OH)]a_1 + [k'_2 + k_2(OH)]a_2 + [k'_3 + k_3(OH)](OH)\} \quad (10)$$

$$-\frac{da_1}{dt} = 2a_1e[k_1(OH) + k'_1)] \quad (11)$$

$$\frac{da_2}{dt} = e\{[k'_1 + k_1(OH)]a_1 + [k'_2 + k_2(OH)]a_2\} \quad (12)$$

$$\frac{d(OH)}{dt} = e\{[k'_1 + k_1(OH)]a_1 + [k'_2 + k_2(OH)]a_2\} \quad (13)$$

where e is the concentration of epoxy equivalents, a_1 is the concentration of primary amine hydrogens, a_2 is the concentration of secondary amine hydrogens, and (OH) is the concentration of hydroxy groups.

When $x_e = (e - e_0)/e_0$, $\alpha = a_1/e_0$, $K_{c1} = k_1e_0^2$, $K'_{c1} = k'_1e_0$, $r = k_2/k_1 = k'_2/k'_1$, and $L = k_3/k_1 = k'_3/k'_1 = K_{c3}/K_{c1}$ are defined and relationships between a_1 and e (integrating the ratio of eqs 10 and 11) and a_1 and a_2 (integrating the ratio of eqs 11 and 12) are found, chemical kinetics for a stoichiometric system may be expressed by[18]

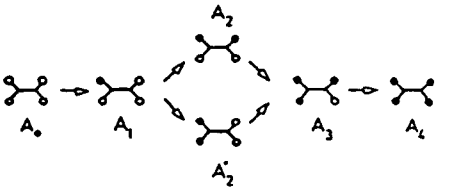

Figure 1. Reaction scheme for the curing of a diamine with a diepoxide. A_i represents a diamine with i reacted amino hydrogens. Key: (●) reacted amino H; (○) unreacted amino H.

$$\frac{dx_e}{dt} = (1 - x_e)[K'_{c1} + K_{c1}F(\alpha)][2(1 - r)\alpha + r\alpha^{r/2} + (2 - r)F(\alpha)L]/(2 - r) \quad (14)$$

$$\frac{d\alpha}{dt} = -2\alpha(1 - x)[K'_{c1} + K_{c1}F(\alpha)] \quad (15)$$

where

$$F(\alpha) = 1 + \frac{(OH)_0}{e_0} - [(1 - r)\alpha + \alpha^{r/2}]/(2 - r) \quad (16)$$

The parameter L is obtained from the fitting of the kinetic model to experimental results. When $L \to 0$, the etherification reaction may be neglected.

Determination of the Diffusion Rate Constants. After vitrification, the reactions become diffusion controlled.

To describe the reaction throughout the whole range of cure, the effect of diffusion control can be incorporated by modifying the rate constant using the Rabinovitch model[27] as suggested by Havlicek and Dusek[23] as follows:

$$\frac{1}{k(x,T)} = \frac{1}{k_c(T)} + \frac{1}{k_d(x,T)} \quad (17)$$

where k is the overall rate constant, k_c is the chemical rate constant (Arrhenius temperature dependence), and k_d is the diffusion rate constant.

Assuming the overall rate constant to follow the empirical Vogel equation, Stütz et al.[28] proposed a different expression:

$$k(x,T) = k_c(T)k_d(x,T) \quad (18)$$

The particularly low activation energies obtained for various epoxy–amine systems[29] cast some doubts about the validity of their expression. Moreover, the Rabinovitch model has the advantage of simply and clearly expressing that the time scale of the reaction equals the time scale of diffusion plus the time scale of the chemical reaction.

The temperature dependence of the diffusion rate constant is governed by relaxation processes in the glassy state. If we take into account that the relaxation time of polymer segments is inversely proportional to the value of k_d, we only need to know the temperature dependence of the molecular relaxation time. Glass transition theories were tested for this purpose.

On one hand, some authors used the free-volume-based Doolittle[30] and Williams–Landel–Ferry (WLF)[31] equations to describe the molecular relaxation time in

the glassy state. Simon and Gillham[19] applied the Doolittle equation to model the DGEBA–trimethylene glycol di-*p*-aminobenzoate diffusion controlled kinetics. For the same epoxy–amine system, Wisanrakkit and Gillham[20] described the molecular relaxation time by a modified form of the WLF equation. From an interesting approach based on dielectric analysis,[24] Deng and Martin[25] characterized the postvitrification stage of DGEBA–diaminodiphenylmethane kinetics using the free-volume relationship between the diffusion coefficient and the dipole relaxation time.

Alternatively, other authors have concentrated on the thermodynamic approach of Gibbs and DiMarzio,[32] who defined a new transition emperature T_2 at which the configurational entropy of the system is zero. Adam and Gibbs[33] extended this concept to correlate relaxational properties to the T_2 and other macroscopic properties. Their treatment considers the probability of a cooperative rearrangement in a fixed subsystem as a function of its size and leads to

$$\ln k_d = \ln k_{d0} - \frac{\ln 2E_d}{\Delta C_p RT \ln \frac{T}{T_g - 50}} \qquad (19)$$

where E_d is the activation energy of the diffusion mechanism and ΔC_p is the discontinuity in the isobaric heat capacity at T_g.

The Adam–Gibbs theory, as the free-volume-based equation, was found to successfully describe the diffusion-controlled kinetics of various epoxy–amine systems.[34]

There is, however, a fundamental difference between the physical concepts on which the free-volume theory and the Adam–Gibbs theory are respectively based. The free-volume theory considers that molecular mobility is only the consequence of free-volume redistribution without overcoming an energy barrier. Differently, in the Adam–Gibbs theory, molecular mobility is assumed to be the consequence of a cooperative rearrangement of structural units due to thermic fluctuations, that permit the overcoming of the energy barrier separating the initial and the final conformation.

So, a good fit of experimental results cannot be a criteria for validating a given theory. Only the analysis of the above mentioned physical concepts can allow conclusions about its accuracy.

Matsuoka et al.[35] pointed out that the free-volume theory is not adequate when trying to predict the relaxation behavior in the nonequilibrium state, whereas the Adam–Gibbs approach based on conformational entropy is a clearly better theory on the basis of experimental evidence. Struik[36] has especially shown that relations related to the free-volume concept, as developed by Cohen and Turnbull,[37] are far from expressing the molecular mobility variation below T_g. Cohen and Turnbull even expressed that the obeying of the hypothesis, on which their concept is developed, imposes weak interactions between neighboring units, i.e. temperatures higher than T_g + 50 K to 100 K. If this conditions is not observed, it is obvious that an energy barrier needs to be taken into account as in the Adam–Gibbs approach.

The preceding inconsistencies do not mean that the free-volume concept is fundamentally invalid, but the relations developed from it have to be reconsidered.

It can also be said that the Adam–Gibbs theory presents some weakness as the assumption of nondependence of T_2 with molecular interactions or mathematical approximations necessary to solve the partition function. But these limitations are never related to the basic philosophy of the theory itself.

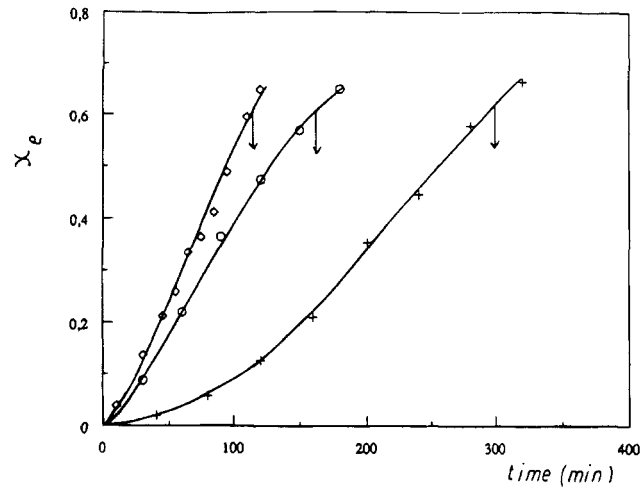

Figure 2. Epoxy conversion vs reaction time at 135 °C for different comonomers: (◇) DGEBA–MDEA; (○) DGEBA–DDS; (+) DGEBA–MCDEA. Arrows (↓) indicate gelation times.

To close this discussion, without challenging the free-volume notion which led to satisfactory formulations for liquids at $T > T_g$, the nonequilibrium state ($T < T_g$) is better described, considering physical concepts, by theories including thermally activated overcoming of an energy barrier.

Results and Discussion

Comparison of the Reactivities of Aromatic Diamines. Figure 2 shows the evolution of epoxy conversion with time at 135 °C for the systems with DDS, MDEA and MCDEA comonomers. Gelation is indicated by an arrow. Although the isothermal cure at 135 °C for DGEBA–MDA was not kinetically characterized (too fast a reaction), a preliminary experiment showed that an insoluble fraction is obtained after approximately 10 min. In order to determine the kinetic rate constants (results will be presented and discussed later), two other cure temperatures, 80 and 160 °C, were investigated for both DDS and MCDEA. Epoxy conversion rises as a function of time and cure temperature, as plotted in Figure 3a (MCDEA) and 3b (DDS). The gelation times are given in Table 2.

It is now possible to compare the reactivities of the diamines, related to their basicity and their steric hindrance, and to understand the effects of their structure.

At the gel point $x_{gel} = 0.60$; from gelation times the following scale of reactivity can be established if the reactivity measured by t_{gel} of MCDEA is considered to be 1 at 135 °C, the others are 1.8 for DDS, 2.6 for MDEA, and 29.5 for MDA.

MDA is known to have a stronger reactivity than DDS. The $-SO_2-$ group has indeed a delaying action on the reactivity of the amine functions because it is a high electron-attracting group which decreases the basicity of the amine, whereas the $-CH_2-$ group is an electron donor. The diethyl ortho-substituted MDEA, which is relatively hindered, is also found to be higher in reactivity than DDS. However, the reactivity of the amine functions appears to be less affected by steric hindrance induced by the electron donor ethyl groups than by the $-SO_2-$ group.

On the other hand, substituted chlorine atoms, due to their high electronegativity, increase the effect of

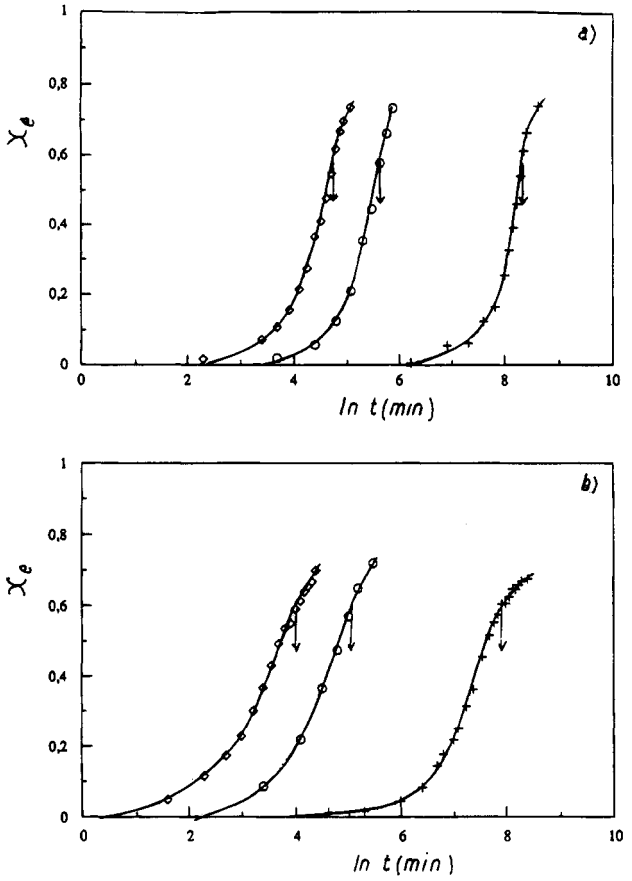

Figure 3. Epoxy conversion vs reaction time at different cure temperatures: (◇) 160 °C; (○) 135 °C; (+) 80 °C. For (a) DGEBA–MCDEA and (b) DGEBA–DDS. Arrows (↓) indicate gelation times.

Table 2. Gelation Time, t_{gel} (min), at Different Cure Temperatures T_c

T_{cure} °C	MDA	MDEA	DDS	MCDEA
80	105		2500	4300
135	10	115	165	300
160			62	120

ethyl groups and MCDEA consequently exhibits the lowest reactivity.

Ratio of Secondary to Primary Amino-Hydrogen Rate Constants, $r = k_2/k_1$. We determined the r values that best fit previously described kinetics results using eq 9. An example of such a determination is shown in Figure 4. To clear the influence of the diamine structure, r was also determined for MDA cured with DGEBA at 80 °C (at this temperature, t_{gel} was 105 min and a wide range of experimental data could thus be obtained). Results are listed in Table 3.

For the aromatic diamines studied, the ratio is found to be lower than unity. This is consistent with experimental conversions at the gel point always higher than $x_{gel} = 0.577$, the theoretical value for a reactivity ratio $r = 1$.

Firstly, we will consider the effect of temperature on the ratio. From the values obtained at different cure temperatures for DDS and MCDEA, no temperature dependence is observed. This agrees with most of the published results[4,5,8,20] in that, if the activation energies for the reaction of epoxy with primary and secondary energies are considered to be the same, the ratio k_2/k_1 is the result of the ratio of frequency factors. As the frequency factor is temperature independent, the ratio of rate constants does not depend on the temperature.

We can now consider the effect of the diamines structure by comparing all the results. Although MDA,

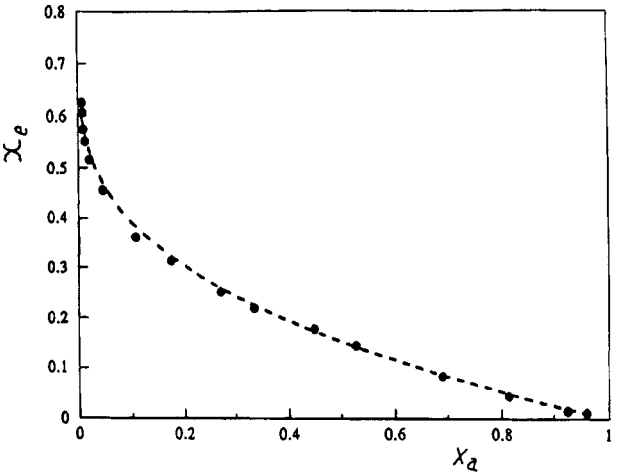

Figure 4. Determination of the ratio k_2/k_1 from kinetic results of DGEBA–DDS at $T_i = 80$ °C using eq 7: (●) experimental; (- - -) adjustment.

Table 3. Ratio of Rate Constants $r = k_2/k_1$ (±0.05) at Different Cure Temperatures

T_c (°C)	DDS	MDA	MDEA	MCDEA
80	0.46	0.65		0.67
135	0.42		0.66	0.64
160	0.51			0.70

MDEA, and MCDEA exhibit very different reactivities, the reactivity ratios are measured to be the same within the range of experimental error. The following conclusions may be drawn: (i) the diethyl groups do not affect the reactivity ratio, as the steric hindrance induced is the same for primary and secondary amines; (ii) the chlorine atoms decrease the basicity of amino groups but do not affect the reactivity ratio.

Concerning MDA, MDEA, and MCDEA, no data are available in the literature.

On the other hand, DDS exhibits a lower reactivity ratio. Its structure is only different from the MDA one by the presence of a $-SO_2-$ group instead of a $-CH_2-$ group. The attractive mesomeric effect of $-SO_2-$ cannot be involved because it exists for both the primary and secondary amines.

A conformational analysis was then run on DDS and MDA molecules using the Sybyl 6.0 molecular modeling package. The conformational energy was calculated as a function of the torsional angles θ_1 and θ_2, defined in Figure 5, around the $-SO_2-$ group in the case of DDS and the $-CH_2-$ group in the case of MDA. The resulting conformational energy maps are given in Figure 6a (DDS) and 6b (MDA). MDA exhibits eight minimal energy conformations M corresponding to (θ_1, θ_2) = [(±110, ±110); (±70; ±70)] whereas DDS exhibits only four corresponding to (θ_1, θ_2) = (±90, ±90). To provide a transition from the minimum M_1 to the minimum M_2 through the ⟨⟨col⟩⟩c, the energy gap is 0.9 kcal·mol^{-1} for MDA compared to 1.6 kcal·mol^{-1} for DDS. Consequently, the MDA higher reactivity ratio was assumed to be the result of the greater number of stable conformations afforded by the $-CH_2-$ group compared to the $-SO_2-$ one. Obviously, more work should be done to confirm this hypothesis, especially the conformational analysis of these substituted diamines with one of their hydrogens reacted. This would, however, require a detailed study.

In the literature, the existing results concerning the magnitude of the substitution effect in DDS are somewhat controversial. On one hand, some authors have reported values ranging from 0.2 to 0.6.[3,17,18] Our result

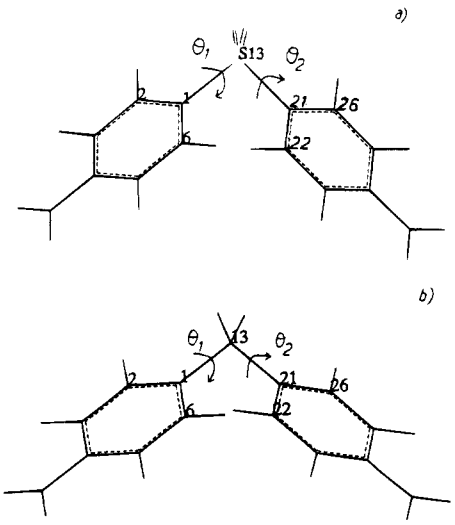

Figure 5. Wire frame views of the minimized conformation: (a) DDS; (b) MDA. Symbols θ_1 and θ_2 stand for the torsional angles C_6, C_1, C_{13}, C_{21} and C_{22}, C_{21}, C_{13}, C_1, respectively.

falls within this range and is pretty close to the 0.4 value found by Bidstrup et al.[17] and Williams et al.[18] On the other hand, other authors have proposed r values close to unity.[8,11] In particular, Grillet et al. found $r = 0.9$; comparatively, this present result seems to be more reliable given that we know in this case it is based on more numerical data and more accurate experiments.

T_g versus Time/Conversion–*TTT* Diagram. The evolutions of T_g versus time at various temperatures are shown in Figure 7a (DGEBA–MCDEA) and 7b (DGEBA–DDS). Besides the previous temperatures of 80, 135, and 160 °C, the reactions were also followed at 30 °C. Kinetic studies at 30 °C are indeed interesting because they can provide information about the reactivity of these systems at a temperature close to the usual stocking conditions.

The vitrification times are indicated by an arrow. At 30 °C, 50 days are needed for DGEBA–DDS to vitrify and 75 days for DGEBA–MCDEA.

Note that the evolution of T_g was measured long after vitrification in order to further model the diffusion-controlled kinetics.

The reevaluated DiBenedetto[38] equation leads to a convenient relationship between the extent of reaction x_e and the glass transition temperature T_g:

$$\frac{T_g - T_{g0}}{T_{g\infty} - T_{g0}} = \frac{\lambda x_e}{1 - (1 - \lambda)x_e} \qquad (20)$$

where T_{g0} is the T_g of the unreacted monomers ($x = 0$), $T_{g\infty}$ is the glass transition of the fully cured network ($x = 1$), and λ is an adjustable parameter.

From an extension of Couchman's approach,[39] Pascault and Williams[40] showed that λ may be estimated by the ratio $\Delta C_{p\infty}/\Delta C_{p0}$ where $\Delta C_{p\infty}$ and ΔC_{p0} are, respectively, the isobaric capacity changes of the fully reacted network and of the initial unreacted mixture.

Parameters involved in eq 20 were determined by DSC measurements. Resulting values for DDS and MCDEA are given in Table 4. The increase of T_g versus x_e using eq 20 is plotted in Figure 8 for both curing agents with experimental results from previous T_g versus time and x_e versus time isothermal analysis. An excellent correlation is observed.

This validated relationship between T_g and x_e can now be a suitable way to determine the gel T_g. This critical temperature denotes the temperature at which gelation

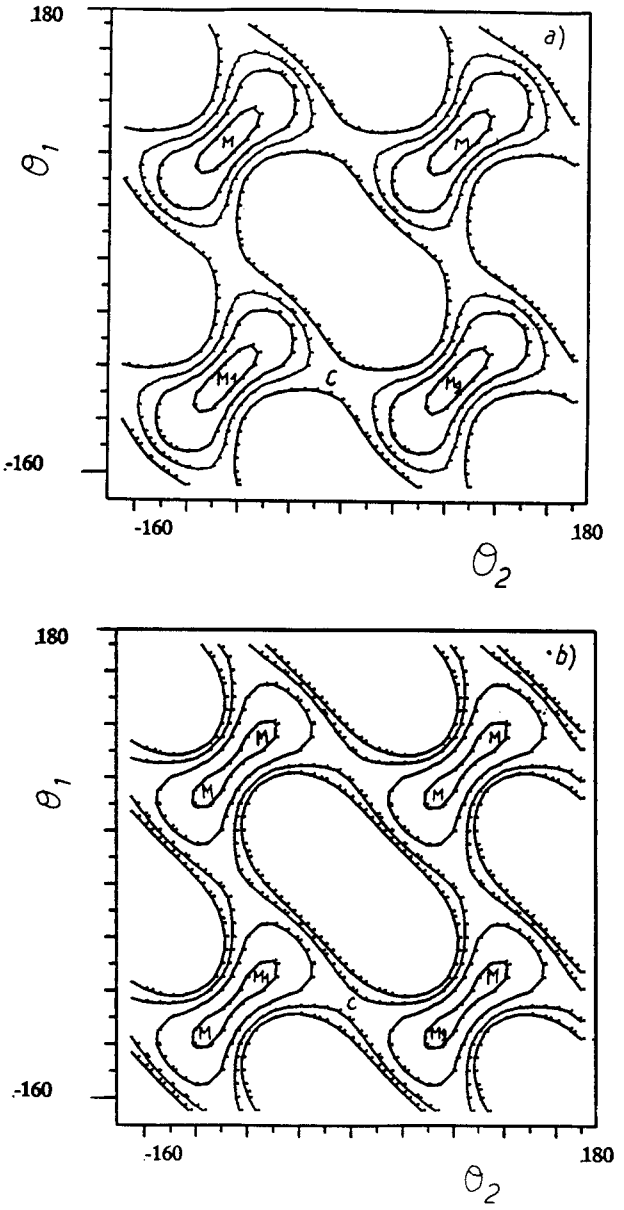

Figure 6. Conformational energies isocontour of (a) DDS and (b) MDA as a function of the torsional angles θ_1 and θ_2. The contour lines are drawn at energies of 3.1, 3.5, 4.0, and 4.5 kcal·mol^{-1} (MDA) and 6.7, 7.0, 8.0, and 8.5 kcal·mol^{-1} (DDS) with respect to the minima M. C stands for the energy gap to overcome to go from the minimum M_1 to another M_2.

and vitrification occur simultaneously. At T_{cure} > gel T_g gelation takes place before vitrification; at T_{cure} < gel T_g vitrification occurs first.

Taking into account the approximation that $x_{gel} = 0.6$, we concurrently obtained

$$\text{gel } T_g = 69 \text{ °C for DGEBA–DDS}$$

$$\text{gel } T_g = 50 \text{ °C for DGEBA–MCDEA}$$

Figure 9 summarizes all the results and presents gelation and vitrification curves in a time–temperature–transformation TTT diagram.[41]

Modeling of the Chemically-Controlled Kinetics of the Epoxy–Amine Reaction. Prior to vitrification, the reaction occurs in the liquid state and the kinetics are mainly controlled by the rate of chemical reaction.

The chemical rate constants, which have an Arrhenius temperature dependence, were determined for DDS and MCDEA from kinetic results at 30, 80, 135, and 160 °C.

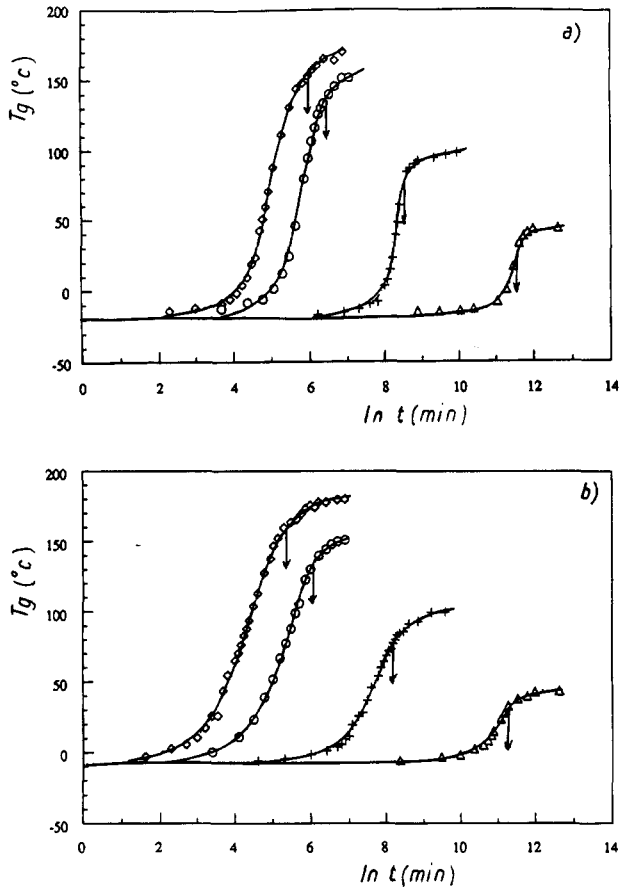

Figure 7. T_g vs reaction time at different cure temperatures: (◇) 160 °C; (m) 135 °C; (+) 80 °C; (△) 30 °C. For (a) DGEBA–MCDEA and (b) DGEBA–DDS. Arrows (↓) indicate gelation times.

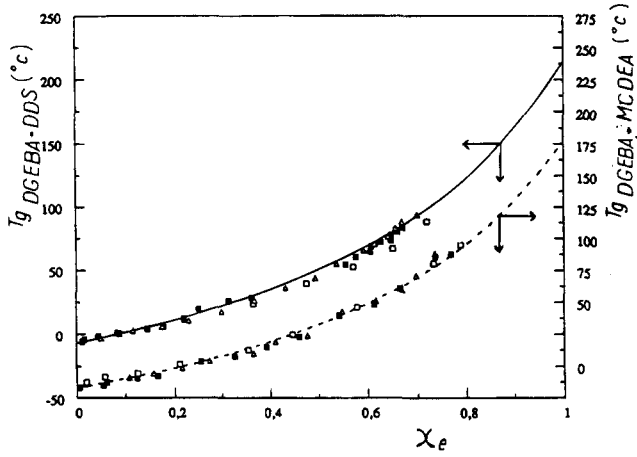

Figure 8. T_g as a function of epoxy conversion. Theoretical curves: (—) DGEBA–DDS; (- -) DGEBA–MCDEA. Experimental data from kinetic studies at different cure temperatures: (■) 80 °C; (□) 135 °C; (△) 160 °C.

Table 4. T_{g0}, $T_{g\infty}$, ΔC_{p0}, and λ for DGEBA–DDS and DGEBA–MCDEA

diamine comonomer	T_{g0} (°C)	$T_{g\infty}$ (°C)	ΔC_{p0} ($J \cdot g^{-1} \cdot k^{-1}$)	$\lambda = (\Delta C_{p\infty}/\Delta C_{p0})$
DDS	−7	214	0.54	0.35
MCDEA	−17	177	0.53	0.34

For this purpose, the Runge–Kutta method was applied with the differential equations (15) and (16). The average values $r = 0.45$ for DDS and $r = 0.65$ for MCDEA were considered. The activation energies for the reaction of epoxy with primary and secondary amino groups were assumed to be the same.

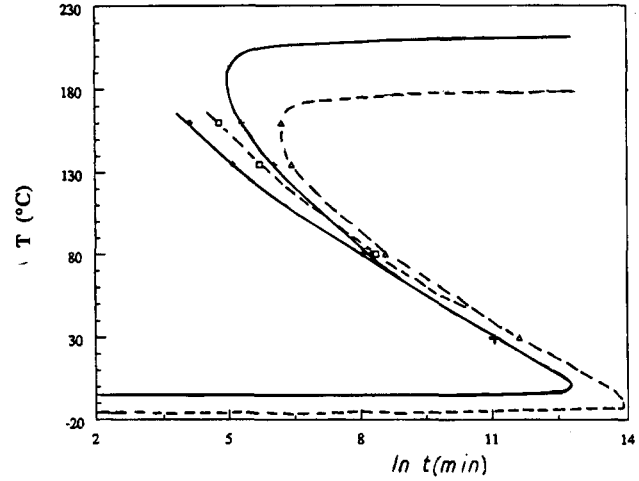

Figure 9. Time–temperature–transformation (*TTT*) diagram for DGEBA with (- - -) MCDEA [(□) gelation, (△) vitrification] and (—) DDS [(♦) gelation, (+) vitrification].

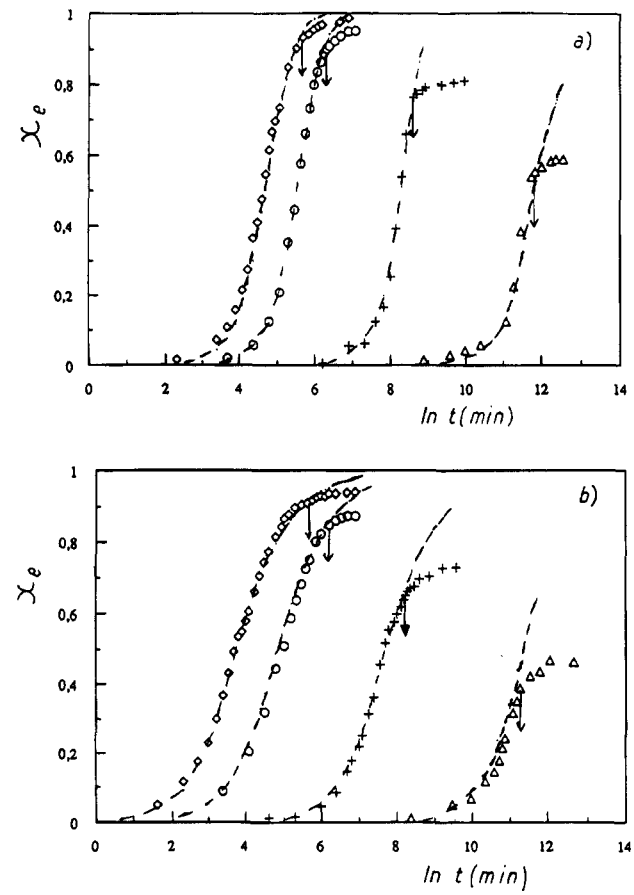

Figure 10. Epoxy conversion vs reaction time at different cure temperatures: (◇) 160 °C; (○) 135 °C; (+) 80 °C; (△) 30 °C; (- - -) chemical model predictions. For (a) DGEBA–MCDEA; (b) DGEBA–DDS. Arrows (↓) indicate vitrification times.

The theoretical conversions of the kinetic model are presented in Figure 10a (DGEBA–DDS) and 10b (DGEBA–MCDEA). In both cases, the kinetic model fits experimental results for the whole previtrification stage, and thereafter typically deviates by overestimating measured conversions. The reaction is then primarily chemically controlled; diffusion control of the reaction becomes influential only after vitrification where the chemical model fails.

For DGEBA–DDS, the etherification reactions were neglected ($K_{c3} = 0$) and the chemical rate constants were found to be

$$K_{c1} = 3.96 \times 10^6 \exp\left(-\frac{7583}{T}\right) \text{min}^{-1} \quad (21)$$

$$K'_{c1} = 1.90 \times 10^5 \exp\left(-\frac{7583}{T}\right) \text{min}^{-1} \quad (22)$$

The autocatalytic mechanism is the main mechanism involved ($K'_{c1}/K_{c1} = 4.8 \times 10^{-2}$). The apparent activation energy, arising from eqs 21 and 22, was $E_c = 63$ kJ·mol^{-1}, in perfect agreement with previously reported results.[8,42]

The situation was somewhat different for the DGEBA–MCDEA system. A good description of the whole previtrification stage at 135 and 160 °C required the consideration of etherification reactions in the kinetic model. If these reactions were not considered, the predictions deviated from experimental results for conversions within the range 0.6–0.7. The etherification reaction is known to be promoted in the case of weakly reactive diamines, which is actually the case of MCDEA. Riccardi and Williams[18] have pointed out that the etherification reaction is only significant at high temperatures and at intermediate and high reaction extents when the primary amine has been sufficiently depleted. IR analysis gave, however, evidence of the presence of this reaction (ether band at 1120 cm^{-1}) for the DGEBA–MCDEA system. The chemical rate constants were found to be

$$K_{c1} = 8.59 \times 10^5 \exp\left(-\frac{7135}{T}\right) \text{min}^{-1} \quad (23)$$

$$K'_{c1} = 1.40 \times 10^3 \exp\left(-\frac{7135}{T}\right) \text{min}^{-1} \quad (24)$$

$$K_{c3} = 2.61 \times 10^2 \exp\left(-\frac{4383}{T}\right) \text{min}^{-1} \quad (25)$$

The noncatalytic rate constant is very low compared to the autocatalytic one ($K'_{c1}/K_{c1} = 1.63 \times 10^{-3}$). The noncatalytic mechanism can then be neglected.

The resulting apparent activation energies were $E_{c1} = 59.9$ kJ·mol^{-1} and $E_{c3} = 36.4$ kJ·mol^{-1}. The value obtained for E_{c3} is very low compared to some results from the literature (80–90 kJ·mol^{-1}), but it results from only two cure temperatures. Other experiments at different T_c's would be obviously desirable to obtain a more accurate value.

Modeling of the Diffusion-Controlled Kinetics of the Epoxy–Amine Reaction. The Rabinovitch model was used to integrate the effect of diffusion control after vitrification.

Considering the effect of diffusion control by the Adam–Gibbs equation (eq 19), the calculations are compared to experimental results in Figure 11a (DGEBA–DDS) and 11b (DGEBA–MCDEA). After vitrification, the variations of ΔC_p are very weak so that ΔC_p was assumed to be constant in calculations. The whole kinetic system, even after vitrification, is then satisfactorily described using such a modified rate constant.

The resulting activation energies of the diffusion mechanism were respectively found to be $E_d = 3.6$ kJ·mol^{-1} for DGEBA–DDS and $E_d = 7.7$ kJ·mol^{-1} for DGEBA–MCDEA. In comparison, the activation energies for diffusion in polymers are in the range 5–20 kJ·mol^{-1}. The lowest known activation energies are those from rotation of C–C bonds with 3–5 kJ·mol^{-1}.

Our values fall near the borders of these two kinds of molecular motions. A rotation around a C–C bond may then be sufficient to allow linked functions to react after vitrification.

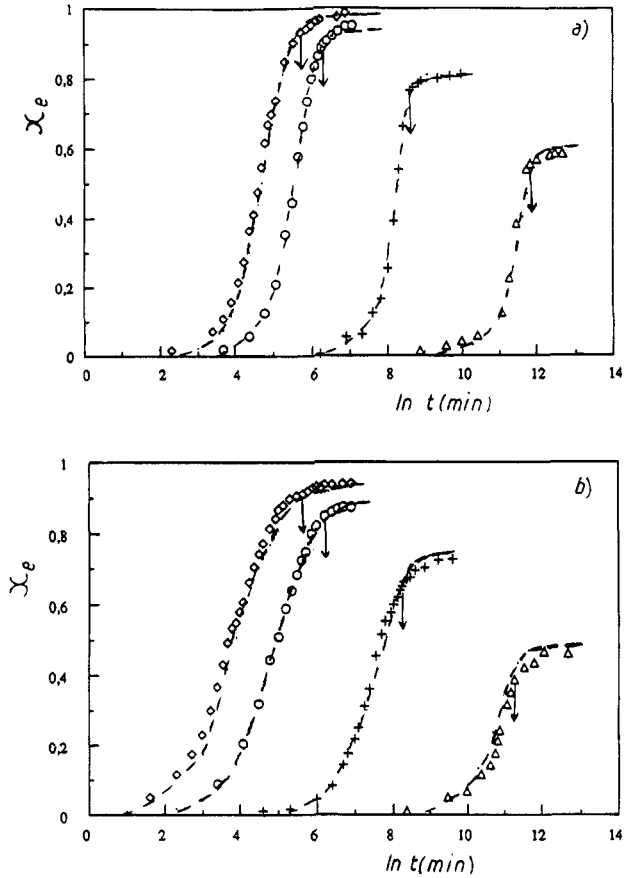

Figure 11. Epoxy conversion vs reaction time at different cure temperatures: (◇) 160 °C; (○) 135 °C; (+) 80 °C; (△) 30 °C; (- - -) diffusion model predictions. For (a) DGEBA–MCDEA; (b) DGEBA–DDS. Arrows (↓) indicate vitrification times.

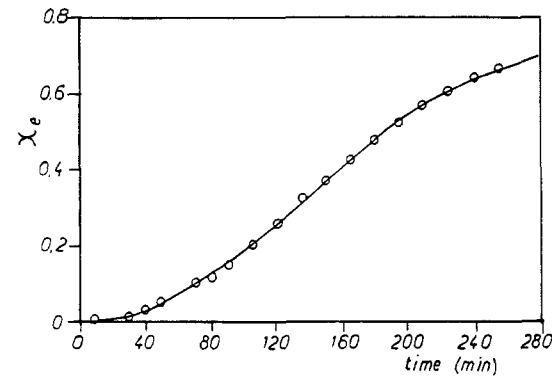

Figure 12. Epoxy conversion vs reaction time for the system DGEBA–30% per mole DDS/70% per mole MCDEA cured at $T_i = 135$ °C: (○) experimental; (- - -) model predictions.

Application of Kinetic Models for Hardener Blends. The combination of two diamines with different reactivities can be an attractive way to get intermediate-range reactivities. This can be especially useful for studies on phase separation.

The reaction kinetics of a stoichiometric mixture of DGEBA with 30% (per mol) DDS and 70% MCDEA were studied at 135 °C. The kinetics were concurrently modeled using previously determinated kinetic rate constants. For the range of conversion studied, the etherification reactions were neglected. An excellent agreement is observed between the experimental and predicted epoxy conversions (Figure 12).

Knowing the kinetic rate constants of two diamines with an epoxy monomer, the reaction kinetics of the

epoxy monomer cured with any mixture of those diamines can be predicted. The reactivity of the blend can be ajusted by changing the proportion of each diamine. This could be extended to other binary diamine mixtures.

Conclusions

(i) The reactivities of various aromatic diamines were compared and correlated to their chemical structures. The following order of reactivity was found:

$$\text{MDA} > \text{MDEA} > \text{DDS} > \text{MCDEA}$$

(ii) The effects of temperature and chemical structure of the diamines on the ratio of secondary to primary amino-hydrogen rate constants were discussed. From the values obtained at different cure temperatures for DDS and MCDEA, no temperature dependence was observed. Although MDA, MDEA, and MCDEA exhibit very different reactivities, their reactivity ratios were measured to be the same, $r = 0.65$. On the other hand, the reactivity ratio of DDS was found to be $r = 0.45$. This lower value may be the result of the lower number of stable conformations afforded by the $-SO_2-$ group than the $-CH_2-$ group.

(iii) DGEBA–DDS and DGEBA–MCDEA kinetics were fully characterized in the way of conversions and T_g measurements with time at different cure temperatures. Reactions were even followed at 30 °C. The relationships between T_g and x_e were validated for both systems. TTT isothermal cure diagrams were introduced to summarize gelation and vitrification results.

(iv) Considering only catalytic and noncatalytic mechanisms, DGEBA–DDS reactions were modeled. Deviation of the predictions from experimental results occurs around vitrification, indicating that the reactions thereafter become diffusion controlled.

For the DGEBA–MCDEA system, etherification reactions were found to occur and were integrated into the kinetic model. The whole previtrification stage is then satisfactorily described. The Arrhenius-type temperature dependencies of the chemical rate constants are expressed, and the resulting activation energies are given.

(v) The effect of diffusion control was incorporated by modifying the overall rate constant according to the Rabinovitch model. Considering physical concepts, the nonequilibrium state is better described by equations including an activation energy term than by free-volume-based equations. The temperature dependence of the diffusion rate constant has been expressed using the Adam–Gibbs theory. Calculations using such modified rate constants provide a good correlation with the experimental results. Diffusion activation energies were determined.

(vi) The kinetic models have been satisfactorily extended to the isothermal cure of an epoxy with a binary mixture of diamines. This could be of interest for further studies on the phase separation process.

Acknowledgment. We would like to thank the Direction Recherche Etudes et Techniques (DRET) for financial support and G. Schwach for molecular modeling. C.C.R. wishes to thank Foundation Antorchas.

References and Notes

(1) Horie, K.; Hiura, H.; Sauvada, M.; Mika, I.; Kambe, H. *J. Polym. Sci., Polym. Chem. Ed.* **1970**, *8*, 1357.
(2) Dusek, K.; Ilavsky, M.; Lunak, S. *J. Polym. Sci., Polym. Symp.* **1975**, *53*, 29.
(3) Lunak, S.; Dusek, K. *J. Polym. Sci., Polym. Symp. Ed.* **1975**, *53*, 45.
(4) Charlesworth, J. J. *J. Polym. Sci., Polym. Symp. Edn.* **1980**, *18*, 621.
(5) Riccardi, C. C.; Adabbo, H. E.; Williams, R. J. J. *J. Appl. Polym. Sci.* **1984**, *29*, 2481.
(6) Rozenberg, B. A. In *Epoxy resins and composites-I*; Dusek, K., Ed.; Springer: Berlin. *Adv. Polym. Sci.* **1985**, *72*, 113.
(7) Sabra, A.; Lam, T. M.; Pascault, J. P.; Grenier-Loustalot, M. F.; Grenier, P. *Polymer* **1987**, *28*, 1030.
(8) Seung, C. S. P.; Pymm, E.; Sun, H. *Macromolecules* **1986**, *19*, 2922.
(9) Dusek, K.; Bleha, M.; Lunak, S. *J. Polym. Sci. Polym. Chem. Ed.* **1977**, *15*, 2393.
(10) Toussaint, A.; Cuypers, P.; D'Hont, L. *J. Coat. Technol.* **1985**, *57*, 71.
(11) Grillet, A. C.; Galy, J.; Pascault, J. P. *Polymer* **1989**, *30*, 2094.
(12) Verchère, D.; Sautereau, H.; Pascault, J. P.; Riccardi, C. C.; Moschiar, S. M.; Williams, R. J. J. *Macromolecules* **1990**, *23*, 725.
(13) Wang, X.; Gillham, J. K. *J. Appl. Polym. Sci.* **1991**, *43*, 2267.
(14) Min, B. G.; Stachurski, Z. H.; Hodgkin, J. H. *Polymer* **1993**, *34*, 4488.
(15) Charlesworth, J. J. *J. Polym. Sci., Part A* **1987**, *25*, 731.
(16) Johncook, P.; Porecha, L.; Tudgey, G. F. *J. Polym. Sci., Part A* **1985**, *23*, 291.
(17) Bidstrup, S. A.; Macosko, C. W. In *Crosskinked Epoxies*; Sedlacek, B., Kahovec, J., Eds.; Walter de Gruyter: Berlin, 1987; p 359.
(18) Riccardi, C. C.; Williams, R. J. J. *J. Appl. Polym. Sci.* **1986**, *32*, 3445.
(19) Simon, S. L.; Gillham, J. K. *J. Appl. Polym. Sci.* **1992**, *46*, 1245.
(20) Wisanrakkit, G.; Gillham, J. K. *J. Appl. Polym. Sci.* **1990**, *41*, 2885.
(21) Dusek, K. *Polym. Mater. Sci. Eng.* **1983**, *49*, 378.
(22) Simon, S. L.; Gillham, J. K. *J. Appl. Polym. Sci.* **1993**, *47*, 461.
(23) Havlicek, I.; Dusek, K. In *Crosskinked Epoxies*, Sedlacek, B., Kahovec, J., Eds.; Walter de Gruyter: Berlin, 1987; p 359.
(24) Deng, Y.; Martin, C. *Macromolecules* **1994**, *27*, 5141.
(25) Deng, Y.; Martin, C. *Macromolecules* **1994**, *27*, 5147.
(26) Lin, Y. G.; Sautereau, H.; Pascault, J. P. *J. Appl. Polym. Sci.* **1986**, *32*, 4585.
(27) Rabinovitch, E. *Trans. Faraday Soc.* **1937**, *33*, 1225.
(28) Stütz, H.; Mertes, J.; Neubecjer, K. *J. Polym. Sci., Part A* **1993**, *31*, 1879.
(29) Stütz, H.; Mertes, J. *J. Polym. Sci., Part A* **1993**, *31*, 2031.
(30) Doolittle, A. K. *J. Appl. Phys.* **1951**, *22*, 171.
(31) Williams, M. L.; Landel, R. F.; Ferry, J. D. *J. Am. Chem. Soc.* **1955**, *77*, 3701.
(32) Gibbs, J. H.; DiMarzio, E. A. *J. Chem. Phys.* **1958**, *28*, 373.
(33) Adam, G.; Gibbs, J. H. *J. Chem. Phys.* **1965**, *43*, 139.
(34) Havlicek, V.; Votja, V.; Kästener, S.; Schlosser, E. *Makromol. Chem.* **1978**, 179, 2467.
(35) Matsuoka, S.; Quan, X.; Bair, H. E.; Boye, D. J. *Macromolecules* **1989**, *22*, 4093.
(36) Struik, L. C. E. *Physical ageing in amorphous polymer and other materials*; Elsevier: Amsterdam, 1978.
(37) Cohen, M. H.; Turnbull, D. *J. Chem. Phys.* **1959**, *31*, 1164.
(38) Nielsen, L. E. *J. Macromol. Sci. Rev. Macromol. Chem.* **1969**, *C3*, 69.
(39) Couchman, P. R. *Macromolecules* **1987**, *20*, 1712.
(40) Pascault, J. P.; Williams, R. J. J. *J. Polym. Sci., Part B* **1990**, *28*, 85.
(41) Gillham, J. K. *J. Appl. Polym. Sci.* **1973**, *17*, 2067.
(42) Haran, D.; Grenier-Loustalot, M. F. In *Journées Nationales des Composites 5*; Bathias, C., Menkes, D., Eds.; Pluralis: Paris, 1986; p 503.

MA9503625